

Doping Human Serum Albumin with Retinoate Markedly Enhances Electron Transport across the Protein

Nadav Amdursky,^{†,‡} Israel Pecht,[§] Mordechai Sheves,^{*,‡} and David Cahen^{*,†}

Departments of [†]Materials and Interfaces, [‡]Organic Chemistry, and [§]Immunology, Weizmann Institute of Science, Rehovot 76100, Israel

Supporting Information

ABSTRACT: Electrons can migrate via proteins over distances that are considered long for nonconjugated systems. The nanoscale dimensions of proteins and their enormous structural and chemical flexibility makes them fascinating subjects for exploring their electron transport (ETp) capacity. One particularly attractive direction is that of tuning their ETp efficiency by “doping” them with small molecules. Here we report that binding of retinoate (RA) to human serum albumin (HSA) increases the solid-state electronic conductance of a monolayer of the protein by >2 orders of magnitude for RA/HSA \geq 3. Temperature-dependent ETp measurements show the following with increasing RA/HSA: (a) The temperature-independent current magnitude of the low-temperature (<190 K) regime increases significantly (>300-fold), suggesting a decrease in the distance-decay constant of the process. (b) The activation energy of the thermally activated regime (>190 K) decreases from 220 meV (RA/HSA = 0) to 70 meV (RA/HSA \geq 3).

Bridging the worlds of biology and solid-state electronics presents a fascinating challenge.^{1–4} One approach to achieve this explores the use of biomolecules as electron transport (ETp) materials.² Indeed, diverse biological macromolecules, from proteins^{5–9} and peptides¹⁰ to DNA^{11–13} and peptide-nucleic acids,^{14,15} have been studied as such, using scanning probe (conducting probe atomic force or tunneling) microscopy or measurements via molecules sandwiched between macroscopic electrodes.^{2,6–9,16} Most studied proteins are those having biological electron transfer (ET) function, such as azurin,^{7,9,17,18} cytochrome *c/b*,^{16,19,20} or plastocyanin.^{21,22} Heller and co-workers^{23–25} showed that electrical communication between enzymes and metal or carbon electrodes can be achieved by derivatizing the proteins with metal-containing electron-relay molecules so that currents are carried between the enzyme’s redox center and the electrode.

Our interests are in understanding if and how electrons can be carried *across the entire protein* and how that transport can be modulated. One factor that can modulate and increase ETp via the protein is the presence of embedded cofactors.

We have recently shown, using macroscopic contacts, that bacteriorhodopsin (bR), a protein that does not have a natural ET function but contains the covalently bound cofactor retinal, has a room-temperature ETp efficiency similar to that of ET proteins.^{7,26} However, proteins devoid of any cofactor, such as

apo-azurin and serum albumin as well as washed apo-bR, exhibit an order of magnitude lower ETp efficiency than, e.g., the ET protein azurin.^{7,18} Here we show that ETp via human serum albumin (HSA), a protein that lacks any cofactor, increases by over 2 orders of magnitude upon binding non-covalently (“doping with”) 3 equivalents of deprotonated retinoic acid, i.e., retinoate (RA). RA is a close derivative of the bR cofactor (retinal) and has a biological role in the growth and development of embryos.²⁷ We chose to study HSA because of its extraordinary capacity to bind small, mainly hydrophobic molecules.²⁸ In this context, Mentovich et al.²⁹ showed how adding C₆₀ to bovine serum albumin (BSA) changes the gate voltage dependence of a BSA-based transistor. We used the all-trans isomer of RA, due to its relatively high affinity to HSA, with an average binding constant of $3.3 \times 10^5 \text{ M}^{-1}$, and as it has no known effect on the proteins’ conformation.^{30–34} HSA has been suggested to bind up to 3 equiv of RA,^{30–34} but as no three-dimensional structure of an HSA-RA complex is available, the locations of the RA binding sites within HSA are not agreed on. N’Soukpoe-Kossi et al.³⁴ suggested that RA binding sites are those known for long-chain fatty acids.³⁵ Maiti et al.³² proposed, based on molecular dynamics docking simulations, one hydrophobic site between subdomains IIA and IIIA, while Belatik et al.³⁰ suggested the site of subdomain IB (one of the binding sites for long-chain fatty acids) to be the main RA binding site (cf. Figure S1 in the Supporting Information).

The addition of RA (stock solution in ethanol) to HSA (aqueous PBS buffer, pH 8) leads to its binding, monitored by UV–vis absorption (Figure 1a) and photoluminescence (Figure 1b) spectroscopies. As illustrated in Figure 1a, we observed a gradual increase in absorption ($\lambda_{\text{max}} = 346 \text{ nm}$, ascribed to RA³³) as the ratio of ligand to protein (L/P), i.e., RA/HSA, was increased, suggesting RA-HSA complex formation, and that RA binds as retinoate. As can also be seen in Figure 1a, at L/P = 4, a second band (at $\sim 405 \text{ nm}$), red-shifted from the main band (346 nm) appears. This second band is ascribed to retinoic acid.³³ The increase in the 346 nm band intensity at L/P = 4 suggests that a fourth RA might bind to HSA, but due to the appearance of the second absorption band at $\sim 405 \text{ nm}$, we can conclude that the pK_a of this binding site is somewhat increased in comparison to those of the other binding sites. However, and more important to the scope of this Communication (as will be shown later), the fourth equivalent of RA hardly affects the ETp characteristics. Further

Received: September 9, 2012

Published: October 23, 2012

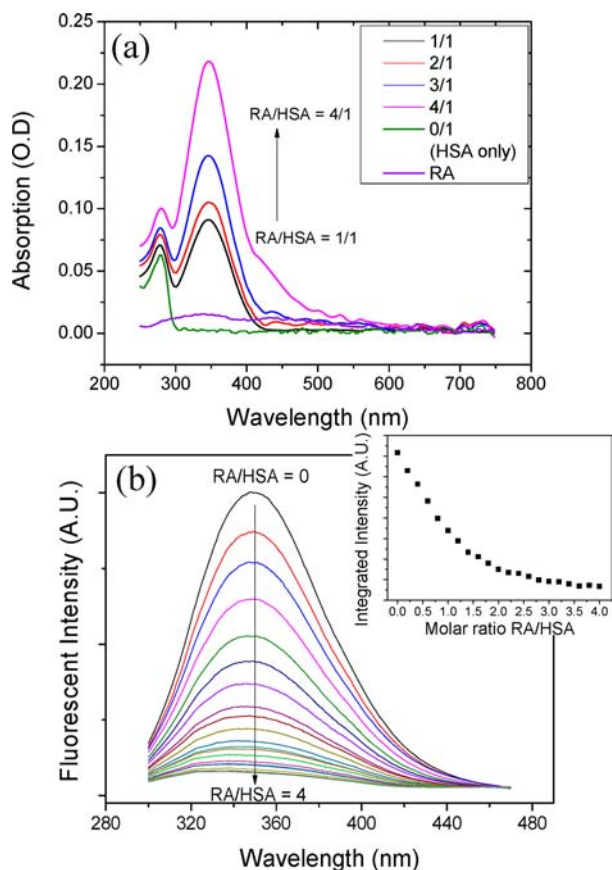


Figure 1. (a) Optical UV–vis absorption (the concentration of RA [purple curve] is equal to that of the first equivalent) and (b) emission ($\lambda_{\text{ex}} = 290$ nm) spectra of HSA-RA complexes at different L/P ratios at pH = 8. The inset shows the integrated fluorescence intensity as a function of the L/P molar ratio.

evidence for RA being the main species bound to HSA is derived from the absorption spectra of RA-HSA complexes with different L/P ratios at different pH values (Figure S2 and supplemental text), which show lower absorption at low pH's (pH = 6–7) than at high pH's (pH = 8–9).

The binding of RA to HSA also causes emission quenching of the HSA tryptophan residue (W_{214} ; Figure 1b). As can be seen in the inset, the decrease in the emission intensity starts to level off only after the addition of the third equivalent of RA, indicating that the first three bound RA molecules are located in close proximity to the tryptophan residue of HSA. As initially observed by Karnaukhova,³¹ RA, which is an optically inactive molecule, exhibits a circular dichroism (CD) band as it binds to HSA, induced by its chiral binding site. In order to further validate our successful binding of RA to HSA, we also observed this CD band (300–400 nm) as we added RA to HSA solution (Figure S3).

Monolayers of HSA alone and of its complexes with RA at different L/P ratios were prepared on a Si surface for ETp measurements. The protocol used was the same as that previously employed for studies of BSA.⁷ The similarity of surface coverage by HSA at different L/P ratios was verified optically by ellipsometry, yielding an optical thickness of 17–20 Å. In addition, atomic force microscopy (AFM) indicated similar surface morphology of the different surfaces, comparable to that found for surfaces of BSA monolayers (Figure S4).⁷ The low optical thickness and surface roughness (rms of 1.6 nm)

suggest that HSA binds with its large-area face to the surface, while the small-area face is the height of the layer (cf. Figure S5). To further validate that the protein retains its structure also in dry configuration, we measured the CD spectra of dry layers of HSA and HSA-RA on quartz and compared them to those in aqueous solution (Figure 2a). As the figure clearly suggests, the protein retains its structure in a dry film configuration.

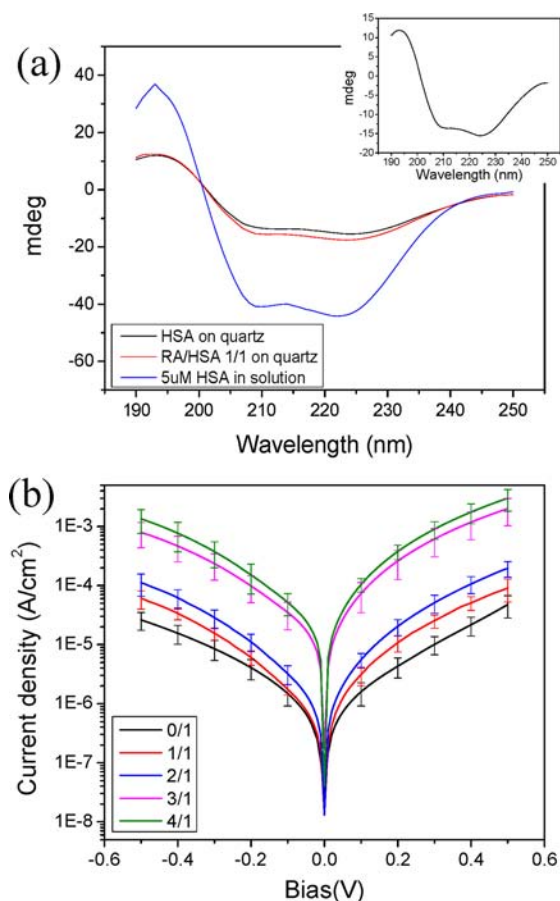


Figure 2. Solid-state characterization of RA/HSA. (a) CD spectra of HSA and RA/HSA in solution (blue curve) and in dry film. The inset shows a magnification of the spectrum of HSA on quartz. (b) Current density–voltage curves of HSA-RA complexes with L/P = 0–4, at room temperature.

While surface coverage and morphology with different L/P values were similar, the ETp efficiency at room temperature (Figure 2b) showed up to nearly a 2 orders of magnitude increase with increasing equivalents of bound RA. The main increase (an order of magnitude) was observed upon binding the third equivalent, while addition of the fourth one gave only a small further increase. This increase in current magnitude is still much lower than if only RA was covering the surface (Figure S6), thus supporting our contention that the RA is still bound to the protein in the dry monolayer configuration.

The common convention for the ET mechanism(s) via helical peptides/proteins (as HSA) can be described by either a coherent process (described by superexchange or tunneling) or hopping.^{36,37} To investigate which mechanism is dominant, one should change the temperature of the environment. Hopping will result in a thermally activated process, while superexchange or tunneling has a low or even no dependence of the

temperature. In order to investigate the ETp mechanism, we studied the change in the current density as a function of temperature (Figure 3a). As can be seen in the figure, all curves

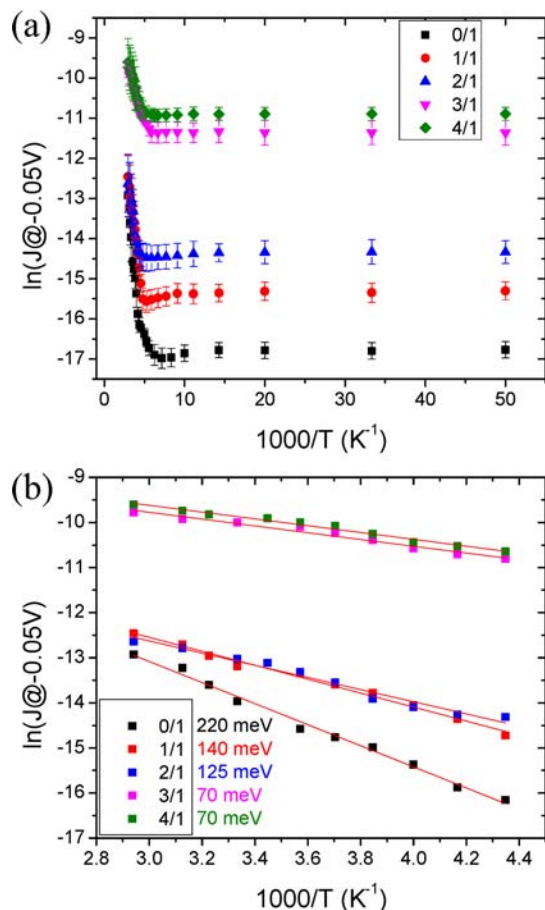


Figure 3. ETp temperature dependence. (a) Current density at -50 mV as a function of temperature over the range of 20–340 K. (b) Zoom-in of the thermally activated regime (230–340 K), showing also the calculated activation energies for each L/P ratio.

exhibit a temperature-independent regime at low temperatures (<190 K) and a thermally activated regime at higher temperatures (≥ 190 K). The magnitude of the current densities and their change as a function of temperature are quite similar for HSA and BSA (Figure S7). The current densities across the proteins can be expressed in the following different forms for the temperature-independent regime, J_{TI} , and for the thermally activated regime, J_{TA} :^{26,38,39}

$$J_{TI} \propto \exp(-\beta l)$$

$$J_{TA} \propto \exp(-E_a/k_B T) \quad (1)$$

where β is the distance-decay constant of ETp, l is the geometrical separation of the electrodes across which ETp takes place, E_a is the activation energy for the thermally activated ETp, k_B is the Boltzmann constant, and T is the absolute temperature. The dominant process at a given temperature determines the observed current density. We will now discuss the effect of binding RA to HSA on ETp in these two regimes.

At low temperatures, where J_{TI} dominates, we find a ~ 330 -fold increase in current densities for the HSA complex with 3 equiv of RA compared to those of HSA alone. The left

proportionality of eq 1 implies that the change in the current density can be explained either by a change in β (assuming that the distance between the electrodes remains the same) or by the pre-exponential factor (not shown in the proportionality), which refers to the coupling matrix of the ETp process via the electrode–protein–electrode system. While we cannot estimate the change in the coupling matrix, the similarity in the junction configurations and the constant separation distance between the electrodes favors β as the main parameter that changes. With this assumption, the increase in temperature-independent current densities can be expressed as a result of a decrease in β values:

$$\frac{J_{TI,0}}{J_{TI,3}} = \frac{H \exp(-\beta_0 l)}{H \exp(-\beta_3 l)} = 3 \times 10^{-3} \xrightarrow{l \approx 37 \text{ \AA}}$$

$$\beta_3 [\text{\AA}^{-1}] = \beta_0 - 0.16 \quad (2)$$

Here H is the coupling matrix and $J_{TI,n}$ and β_n are the current density in the temperature-independent regime and the distance-decay constant at $L/P = n$, respectively. For the calculation we took the thickness of the protein monolayer (perpendicular to the surface), i.e., the maximal distance across which ETp occurs, to be ~ 37 Å, deduced from the three-dimensional structure of the protein (PDB ID: 1E7I, Figure S5), and also illustrated by the z -axis of the AFM image (Figure S4). In a similar way we can calculate that $\beta_2 = \beta_0 - 0.07$ and $\beta_1 = \beta_0 - 0.05$. We assume that in this temperature regime ETp occurs by tunneling, also referred to as superexchange, provided by the bound RA, and even more so with several proximally bound RAs, within HSA. The presence of RA lowers the energy levels involved in the ETp process in a manner similar to that observed in redox proteins,⁴⁰ in line with the decrease in β values.

Binding RA to HSA also affects the ETp behavior in the high-temperature regime, where thermally activated ETp is observed (current density described by J_{TA} as in eq 1), with clear differences in the currents' temperature dependence at different L/P ratios. Plots of $\ln(J_{TA})$ vs T^{-1} are linear (Arrhenius plots; Figure 3b) and show that the activation energy, E_a , decreases as L/P increases. Here, too, it is reasonable to assume that the introduction of several RAs lowers the energy barriers for the non-adiabatic ETp process, corresponding to shallower diabatic curves and lower reorganization energies, which consequently cause a decrease in the observed activation energy.

The large increase in current density through the protein monolayer as a function of RA binding is remarkable, in particular because the doped protein has no known electron- or charge-transfer role in nature. This emphasizes the crucial role of any bound cofactor in the ETp via proteins. It also suggests that a protein can serve as a framework for efficient ETp, upon binding an appropriate cofactor, irrespective of the protein's natural function. In this context, we note that the current density (at 0.05 V) through the doped HSA monolayer (at $L/P = 3$) is even slightly higher, especially in the low-temperature regime, than through bR, a natural retinal-containing protein,²⁶ or through a natural ET protein, azurin.¹⁸

Heller et al.^{23–25} addressed the problem of producing effective electrical communication between redox enzymes and electrodes and established that this can be achieved by covalent binding of metal-containing electron relay linkers. In our work we studied a distinct question, namely, can the ETp via a

protein be enhanced by *non-covalent* binding (“doping”) of a small, conjugated molecule within a polypeptide matrix?

In conclusion, we discovered that the ETP via a solid-state monolayer of HSA increases dramatically as a result of doping it with up to 3 equiv of RA. The increase in ETP with increasing L/P can be interpreted as a change in ETP parameters. This change is expressed as a decrease in both the distance-decay constant of the temperature-independent ETP at low temperatures and the activation energy of the temperature-dependent ETP at higher temperatures. The marked increase in currents caused by RA doping of HSA confirms and significantly extends our earlier tenet that proteins can behave as molecular wires upon cofactor binding. The ability to markedly enhance the electrical conductivity of a protein monolayer over a significant range may be of interest for using proteins as ETP mediators in future bioelectronic device structures, such as biosensors and as biocompatible electronic charge-carrying elements.

■ ASSOCIATED CONTENT

■ Supporting Information

Experimental procedures, protein structure with the possible binding sites, additional UV–vis spectra, CD spectroscopy and additional text, AFM images, I – V curve of RA and I – V – T of BSA. This material is available free of charge via the Internet at <http://pubs.acs.org>.

■ AUTHOR INFORMATION

Corresponding Author

david.cahen@weizmann.ac.il; mudi.sheves@weizmann.ac.il

Notes

The authors declare no competing financial interest.

■ ACKNOWLEDGMENTS

N.A. thanks the Clore program for financial support. We thank the Minerva Foundation (Munich) for partial support. M.S. holds the Katzir-Makineni Chair in Chemistry. D.C. holds the Schaefer Chair in Energy Research.

■ REFERENCES

- (1) Berggren, M.; Richter-Dahlfors, A. *Adv. Mater.* **2007**, *19*, 3201.
- (2) Davis, J. J.; Morgan, D. A.; Wrathmell, C. L.; Axford, D. N.; Zhao, J.; Wang, N. *J. Mater. Chem.* **2005**, *15*, 2160.
- (3) Privman, M.; Tam, T. K.; Pita, M.; Katz, E. *J. Am. Chem. Soc.* **2009**, *131*, 1314.
- (4) Wise, K. J.; Gillespie, N. B.; Stuart, J. A.; Krebs, M. P.; Birge, R. R. *Trends Biotechnol.* **2002**, *20*, 387.
- (5) Inkpen, M. S.; Albrecht, T. *ACS Nano* **2012**, *6*, 13.
- (6) Ron, I.; Pecht, I.; Sheves, M.; Cahen, D. *Acc. Chem. Res.* **2010**, *43*, 945.
- (7) Ron, I.; Sepunaru, L.; Itzhakov, S.; Belenkova, T.; Friedman, N.; Pecht, I.; Sheves, M.; Cahen, D. *J. Am. Chem. Soc.* **2010**, *132*, 4131.
- (8) Xu, D.; Watt, G. D.; Harb, J. N.; Davis, R. C. *Nano Lett.* **2005**, *5*, 571.
- (9) Zhao, J. W.; Davis, J. J.; Sansom, M. S. P.; Hung, A. *J. Am. Chem. Soc.* **2004**, *126*, 5601.
- (10) Scullion, L.; Doneux, T.; Bouffier, L.; Fernig, D. G.; Higgins, S. J.; Bethell, D.; Nichols, R. J. *J. Phys. Chem. C* **2011**, *115*, 8361.
- (11) Hartwich, G.; Caruana, D. J.; de Lumley-Woodyear, T.; Wu, Y. B.; Campbell, C. N.; Heller, A. *J. Am. Chem. Soc.* **1999**, *121*, 10803.
- (12) Olofsson, J.; Larsson, S. *J. Phys. Chem. B* **2001**, *105*, 10398.
- (13) Shao, F. W.; Barton, J. K. *J. Am. Chem. Soc.* **2007**, *129*, 14733.
- (14) Paul, A.; Watson, R. M.; Wierzbinski, E.; Davis, K. L.; Sha, A.; Achim, C.; Waldeck, D. H. *J. Phys. Chem. B* **2010**, *114*, 14140.
- (15) Venkatramani, R.; Davis, K. L.; Wierzbinski, E.; Bezer, S.; Balaeff, A.; Keinan, S.; Paul, A.; Kocsis, L.; Beratan, D. N.; Achim, C.; Waldeck, D. H. *J. Am. Chem. Soc.* **2011**, *133*, 62.
- (16) Della Pia, E. A.; Elliott, M.; Jones, D. D.; Macdonald, J. E. *ACS Nano* **2012**, *6*, 355.
- (17) Davis, J. J.; Wrathmell, C. L.; Zhao, J.; Fletcher, J. *J. Mol. Recognit.* **2004**, *17*, 167.
- (18) Sepunaru, L.; Pecht, I.; Sheves, M.; Cahen, D. *J. Am. Chem. Soc.* **2011**, *133*, 2421.
- (19) Bortolotti, C. A.; Borsari, M.; Sola, M.; Chertkova, R.; Dolgikh, D.; Kotlyar, A.; Facci, P. *J. Phys. Chem. C* **2007**, *111*, 12100.
- (20) Davis, J. J.; Peters, B.; Xi, W. *J. Phys.: Condes. Matter* **2008**, *20*, No. 374123.
- (21) Hope, A. B. *Biochim. Biophys. Acta: Bioenerg.* **2000**, *1456*, 5.
- (22) Sigfridsson, K. *Photosynth. Res.* **1998**, *57*, 1.
- (23) Heller, A. *Acc. Chem. Res.* **1990**, *23*, 128.
- (24) Degani, Y.; Heller, A. *J. Phys. Chem.* **1987**, *91*, 1285.
- (25) Degani, Y.; Heller, A. *J. Am. Chem. Soc.* **1988**, *110*, 2615.
- (26) Sepunaru, L.; Friedman, N.; Pecht, I.; Sheves, M.; Cahen, D. *J. Am. Chem. Soc.* **2012**, *134*, 4169.
- (27) Duester, G. *Cell* **2008**, *134*, 921.
- (28) Fasano, M.; Curry, S.; Terreno, E.; Galliano, M.; Fanali, G.; Narciso, P.; Notari, S.; Ascenzi, P. *IUBMB Life* **2005**, *57*, 787.
- (29) Mentovich, E.; Belgorodsky, B.; Gozin, M.; Richter, S.; Cohen, H. *J. Am. Chem. Soc.* **2012**, *134*, 8468.
- (30) Belatik, A.; Hotchandani, S.; Bariyanga, J.; Tajmir-Riahi, H. A. *Eur. J. Med. Chem.* **2012**, *48*, 114.
- (31) Karnaukhova, E. *Biochem. Pharmacol.* **2007**, *73*, 901.
- (32) Maiti, T. K.; Ghosh, K. S.; Debnath, J.; Dasgupta, S. *Int. J. Biol. Macromol.* **2006**, *38*, 197.
- (33) Noy, N. *Biochim. Biophys. Acta* **1992**, *1106*, 151.
- (34) N’Soukpoe-Kossi, C. N.; Sedaghat-Herati, R.; Ragi, C.; Hotchandani, S.; Tajmir-Riahi, H. A. *Int. J. Biol. Macromol.* **2007**, *40*, 484.
- (35) Sugio, S.; Kashima, A.; Mochizuki, S.; Noda, M.; Kobayashi, K. *Protein Eng.* **1999**, *12*, 439.
- (36) Lopez-Perez, D. E.; Revilla-Lopez, G.; Jacquemin, D.; Zanuy, D.; Palys, B.; Sek, S.; Aleman, C. *Phys. Chem. Chem. Phys.* **2012**, *14*, 10332.
- (37) Gray, H. B.; Winkler, J. R. *Proc. Natl. Acad. Sci. U.S.A.* **2005**, *102*, 3534.
- (38) Segal, D.; Nitzan, A. *Chem. Phys.* **2002**, *281*, 235.
- (39) Selzer, Y.; Cabassi, M. A.; Mayer, T. S.; Allara, D. L. *Nanotechnology* **2004**, *15*, S483.
- (40) Chi, Q.; Farver, O.; Ulstrup, J. *Proc. Natl. Acad. Sci. U.S.A.* **2005**, *102*, 16203.